Biosystems Engineering (2006) **95** (4), 483–496
doi:10.1016/j.biosystemseng.2006.08.009
AE—Automation and Emerging Technologies

Development of Fuzzy Logic Based Differentiation Algorithm and Fast Line-scan Imaging System for Chicken Inspection

C.-C. Yang; K. Chao; Y.-R. Chen; M.S. Kim; D.E. Chan

Instrumentation and Sensing Laboratory, ARS, USDA, Beltsville, MD, USA 20705-2350;
e-mail of corresponding author: chaok@ba.ars.usda.gov

(Received 13 December 2005; accepted in revised form 22 August 2006; published online 13 October 2006)

A fuzzy logic-based algorithm was developed for a hyperspectral line-scan imaging system for differentiation of wholesome and systemically diseased fresh chickens. The hyperspectral imaging system consisted of an electron-multiplying charge-coupled-device (EMCCD) camera and an imaging spectrograph. The imaging system acquired line-scan images of chicken carcasses as they passed through the pixel-wide vertical linear field of view. The chickens were hung on a closed-loop laboratory processing line moving at a speed of 70 birds per minute. The use of light-emitting-diode (LED) line lights was selected following comparative evaluation of LED and quartz–tungsten–halogen (QTH) line lights. From analysis of wholesome and systemically diseased chicken spectra, four key wavelengths for differentiating between wholesome and systemically diseased chickens were selected: 413, 472, 515, and 546 nm; a reference wavelength at 626 nm was also selected. The ratio of relative reflectance between each key wavelength and the reference wavelength was calculated for use as input image features. A fuzzy logic-based algorithm utilising the image features was developed to identify individual pixels on the chicken surface exhibiting symptoms of systemic disease. Two differentiation methods utilising the fuzzy logic-based algorithm were tested using two separate image sets, the first containing 65 wholesome and 74 systemically diseased chickens, and the second containing 48 wholesome and 42 systemically diseased chickens. The first method achieved 100% accuracy in identifying chickens in both image sets. The second method achieved 96% and 100% accuracy in identifying chickens in the first and second image sets, respectively.
Published by Elsevier Ltd on behalf of IAgrE

1. SEQ CHAPTER Introduction

To ensure food safety and prevent food safety hazards in the inspection process for poultry, egg, and meat products, the Food Safety and Inspection Service (FSIS) of the United States Department of Agriculture (USDA) has implemented the Hazard Analysis and Critical Control Point (HACCP) program throughout the country and has also been testing the HACCP-based Inspection Models Project (HIMP) (USDA, 1996). This project includes a zero tolerance standard for chickens with infectious condition such as septicaemia and toxaemia, which must be removed from the processing line. For poultry plants to meet government food safety regulations while maintaining their competitiveness to satisfy consumer demand, FSIS has required the development of new inspection technologies (USDA, 2005), such as automated computer imaging inspection systems.

There have been several research studies using multispectral imaging systems for chicken carcass inspection. Yang *et al.* (2005b) developed a multispectral imaging system using the 540 nm wavelength for feature calculation and the 610 or 700 nm wavelengths for background removal, which achieved classification accuracies of 95·7% for wholesome and 97·7% for unwholesome chicken carcasses. Park *et al.* (2002) achieved 97·3% to 100% accuracies in identifying faecal- and ingesta-contamination of poultry carcasses using images at the 434, 517, 565, and 628 nm wavelengths. Multispectral images contain spectral and spatial information from the surface of

chicken carcasses, both studies identified as being essential for efficient identification of contamination and systemic disease. Also, this non-destructive method shows potential for on-line inspection at high-speed processing plants.

Park *et al.* (2002) also indicated that proper selection of wavelengths is essential for successful multispectral imaging applications. Other studies have used visible/near-infrared spectroscopy analysis to show that certain wavelengths are particularly useful for the identification of diseased, contaminated, or defective chicken carcasses (Yang *et al.*, 2005a; Chen & Massie, 1993). Once essential features that can increase classification accuracy for chicken inspection have been extracted using a hyperspectral imaging system, it is necessary to implement them into a separate multispectral imaging system in order to achieve fast imaging for online inspection application. Thus, a major challenge is the difficulty of cross-system calibration while implementing configurations and features to a multispectral imaging system for fast imaging (Lawrence *et al.*, 2003). Furthermore, considerable effort is required to ensure that a multispectral imaging system with significantly different hardware and software components can obtain the same results as the hyperspectral imaging system. Therefore, a hyperspectral imaging system that is directly converted to multispectral operation without necessitating significant adaptations provides the ideal implementation of essential features, extracted through hyperspectral imaging, for data-efficient high-speed multispectral classification algorithms.

On the other hand, hyperspectral line-scan imaging systems can be used for surface analysis studies, which is the principal basis for chicken carcass imaging and differentiation. Images collected using hyperspectral line-scan imaging systems have been applied to surface roughness measurement (Bjuggren *et al.*, 1997), rapid acquisition of fluorescence lifetime imaging (Connelly *et al.*, 2001), and prediction of nitrogen and phosphorus content in spring barley (Christensen *et al.*, 2004). From these studies, hyperspectral line-scan imaging systems appear to be well suited for detecting differences in surface reflectance between wholesome and systemically diseased chickens.

Illumination is a critical factor influencing the reflectance recorded by a hyperspectral imaging system (Polder *et al.*, 2002). Every light source has its own intensification characteristics in a specific wavelength range (Keskin *et al.*, 2001). A suitable light source provides high-intensity illumination at key wavelengths by which the objects can be properly identified and distinguished. Since the proper selection of wavelengths is essential for a successful multispectral imaging system application, the selection of an appropriate light source also would be crucial for this application.

A line-scan hyperspectral imaging system was used to acquire line-scan images for developing a differentiation algorithm to identify wholesome and systemically diseased chickens, based on image features created from selected key wavelengths. The main objective of this study was to develop a differentiation algorithm for a fast line-scan imaging system for online differentiation of wholesome and systemically diseased chickens. Line-scan images of wholesome and systemically diseased chickens were acquired using both light-emitting-diode (LED) and quartz–tungsten–halogen (QTH) line lights. Wholesome and systemically diseased chicken spectra were extracted from hyperspectral chicken images and used to evaluate key wavelength selections corresponding to the use of the two types of light. Image features for differentiation were generated from the key wavelengths. An algorithm was developed to detect the Region of Interest for each chicken image. A set of fuzzy logic membership functions was derived using sample areas extracted from the chicken images. Two methods using the fuzzy logic-based algorithm were developed to differentiate systemically diseased chickens from wholesome chickens.

2. Materials and methods

2.1. *Chicken carcass collection*

Eviscerated wholesome and systemically diseased chicken carcasses were identified and collected by USDA FSIS veterinarians at an Allen Family Foods chicken processing plant (Cordova, MD, USA). Chicken carcasses were placed in plastic bags and stored in ice boxes with crushed ice to minimise dehydration. The carcasses were then transported, within 2 h, to the Instrumentation and Sensing Laboratory (ISL, USDA-ARS, Beltsville, MD, USA) for the experiments. The carcasses were collected in batches of 7–20 birds over two separate time spans for the following two image sets: 65 wholesome and 74 systemically diseased chickens were collected from August to September of 2005 for the first image set, and 48 wholesome and 42 systemically diseased chickens were collected in October of 2005 for the second image set. Specifically, systemically diseased chicken carcasses collected for this research showed external symptoms of septicemia or toxaemia. Septicaemia is caused by the presence of pathogenic microorganisms or their toxins in the bloodstream, and toxaemia is the result of toxins produced from cells at a localised infection or from the growth of microorganisms.

2.2. *Hyperspectral line-scan imaging system*

The hyperspectral imaging system consisted of an electron-multiplying charge-coupled-device (EMCCD) camera and an imaging spectrograph. Through a slit in the front of the spectrograph, a collimated light beam from the scanned line is dispersed at a prism-grating-prism device in order to obtain a spectrum where the shortest wavelength is at one end and the longest is at the other end. Therefore, for each scanned line, a two-dimensional image of reflectance intensity is created with spatial position along one axis and spectral wavelength along the other.

In this system, a PhotonMAX 512b EMCCD camera (Princeton Instruments, Roper Scientific, Inc., Trenton, NJ, USA), with thermoelectric air cooling down to −70 °C to keep the dark current stable, was used to acquire spectral images. The camera operates with a 10 MHz, 16 bit digitiser for low-light, high-speed image visualisation, which is essential for online chicken inspection. An ImSpector V10 imaging spectrograph (Spectral Imaging Ltd, Oulu, Finland) was used to produce contiguous spectral images, with a slit width of 50 μm. A Rainbow CCTV S6 × 11 C-mount lens (International Space Optics, S.A., Irvine, CA, USA) was attached to the spectrograph. This compact lens is manufactured with a broadband coating for 400 to 1000 nm.The distance from the lens to the shackle was 584 mm.

Two types of line lights, LED and QTH lights, were evaluated as light sources. For the former, a pair of high-power, broad-spectrum 'white' LED line lights (LL6212, Advanced Illumination, Inc., Rochester, VT, USA) was used. The white light from the LEDs is generated by utilising a blue LED to pump one or more visible light-emitting phosphors integrated into the phosphor-converted LED package. The phosphor then converts most of the blue light into red and green light. The horizontal distance from the lights to the shackle was 292 mm. The distance between the two lights was 254 mm. The current for these LED lights can be adjusted individually for four channels: blue, green, red, and infrared. To produce uniform intensity throughout the spectral range, the current was set at 100 mA for each of the four channels. The camera took images with an absolute multiplication gain of about 1·75 and exposure time of 1 ms. For the QTH lights, a pair of fibre optic line lights (PL800 Dolan-Jenner Industries, Inc., Boxborough, MA, USA) was used. Because the maximum intensity of the QTH lights was lower than that of the LED lights, the QTH lights were positioned closer to each other and to the shackle than the LED lights, and the camera was operated with higher multiplication gain for the QTH lights than for the LED lights. The horizontal distance from the lights to the shackle was 254 mm. The distance between the two lights was 95 mm. The camera acquired images with an absolute multiplication gain of about 3·50 and an exposure time of 1 ms.

The software WinView/32 version 2·5·19·0 (Princeton Instruments, Roper Scientific, Inc., Trenton, NJ, USA) was used to control the hyperspectral imaging system for data acquisition. To increase image acquisition speed, the original image size, 512 by 512 pixels, was reduced by binning. Binning is a process of combining the charges from adjacent pixels in the detector array. For a two-dimensional $m \times n$ image with binning, when m pixels are binned by the number k through the dimension X, the charges from every k pixels along dimension X in the detector array are accumulated as one pixel in the resulting image, and the number of pixels in this dimension is reduced to m/k. The binning process is carried out in the hardware of the camera system, resulting in a reduced number of pixels that is converted and digitised for the computer to process. The time to acquire one line-scan image is reduced, so that the imaging speed of the camera system is increased. The binning setting was determined through trial-and-error to improve image acquisition speed while avoiding loss of critical detail. Empirically, the pixels were binned by two in the spatial dimension, and binned by four in the spectral dimension, reducing the image size to 256 by 128 pixels. Before image collection, a mercury–neon lamp (Oriel Instruments, Stratford, CT, USA) was used for spectral calibration. It was found that, because of natural characteristics of the light source and lens, the intensities from the first 19 and the last 6 spectral channels were too low to be used. Discarding these 25 channels, the remaining 103 spectral channels were retained for image acquisition. Thus, the final line-scan image size was 256 by 103 pixels. *Figure 1* shows the average raw spectra for the mercury–neon pencil light, LED and QTH lights, using a Spectralon diffuse reflectance target (Labsphere, Inc., North Sutton, NH, USA). The lamp of the pencil light contains mercury to dominate the output spectrum and neon as a starter gas. Thus, the output of the pencil light in the first minute of usage is that of neon, and afterwards automatically turns to mercury. The following second-order polynomial regression that was used to calibrate the spectral axis, in which λ is the wavelength in nm and n_c is the spectral channel number, was calculated from the five known wavelength peaks of the mercury and neon spectra labelled in *Fig. 1*.

$$\lambda = 0{\cdot}0161 n_c^2 + 5{\cdot}6051 n_c + 389{\cdot}87 \qquad (1)$$

The correlation coefficient of the linear regression between calibrated and expected wavelengths was

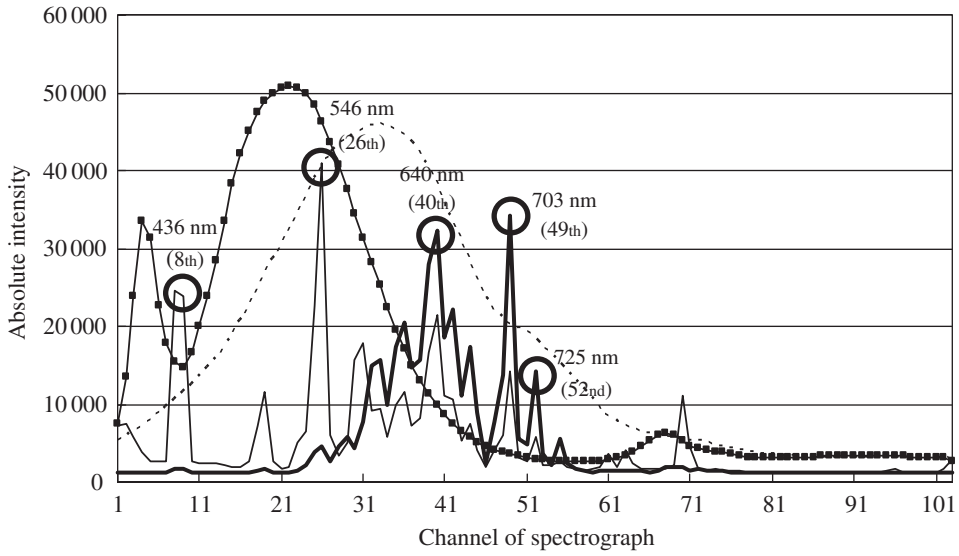

Fig. 1. Spectra for pencil lights (——, mercury; ▬, neon), light-emitting-diode (—■—, LED), and quartz–tungsten–halogen (·····, QTH) line lights using a Spectralon diffuse reflectance target for wavelength calibration

0·9999. From the wavelength calibration, the image spectrum ranged from 395 nm (the first channel) to 1138 nm (the 103rd channel) with an average bandwidth of 7 nm. The 140 mm linear field of view was translated into 256 spatial pixels, with each pixel representing an area of 0·55 by 0·55 mm^2.

2.3. *Image collection and correction procedure*

The laboratory closed-loop pilot-scale processing line was run at 70 birds per minute, reflecting a commonly used speed on poultry plant evisceration lines. The processing line shackles were hung on 152 mm centres and the chickens were hung on these shackles for hyperspectral image acquisition. *Figure 2* shows example images (at the 626 nm wavelength using the LED line lights) of one wholesome and one systemically diseased chicken. When these particular chickens passed through the camera field of view, the hyperspectral imaging system took 130 line-scans of the wholesome bird and 123 line-scans of the systemically diseased bird; the line scans were compiled to form the complete example images as shown in *Fig. 2*. The number of line-scans per bird varied with bird size. After images were taken using one type of line lights, either LED or QTH line lights, the lights were replaced by the other type and the same chickens again passed though the field of view for acquisition of images using the other type of line lights.

The flat field correction was applied to all chicken images acquired. The flat field and dark current reference images were collected first each day, and were

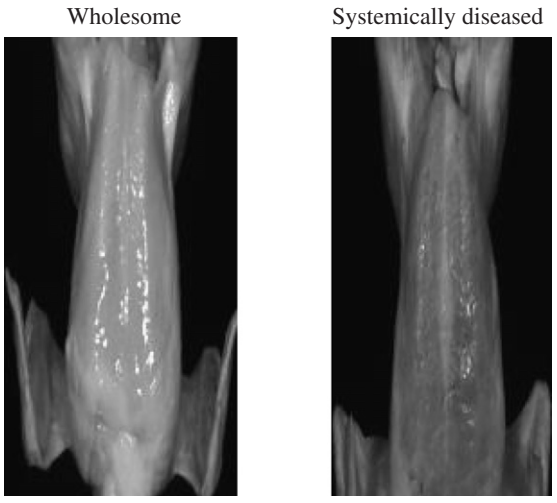

Fig. 2. Example images of wholesome and systemically diseased chickens that combined scanned lines in the 626 nm wavelength by the light-emitting-diode line lights

applied to all line-scan images collected later on the same day. For the flat field image, a Spectralon diffuse reflectance target was used as a calibration target. The Spectralon reference target was hung on a shackle and moved through the field of view. The imaging system acquired 20 line-scans of the target, and the average reflectance from these 20 line-scan images was calculated for the flat field reference image W. The lens was covered completely to take another 20 line-scan images, and the average reflectance from these images was calculated for the dark current reference image D. For

each raw line-scan image I_0, the pixel-based flat field correction was performed to obtain the corrected line-scan image I as follows

$$I = \frac{I_0 - D}{W - D} \quad (2)$$

The relative reflectance in the corrected line-scan image I was used for image analysis and differentiation. A black imaging background was used so that the chicken image could be easily extracted from the background. Empirically, when the relative reflectance was lower than 0·05 at the 626 mm wavelength, the pixel was identified as background and could be discarded.

2.4. *Key wavelength, image feature, and region of interest selections*

From among the 103 wavebands collected by the hyperspectral imaging system, selection of appropriate key wavelengths is crucial for accurate high-speed image acquisition and differentiation. From each carcass image in the first image set, 25 spots were randomly selected from the lower abdomen and breast of the chicken. The average spectrum of 1625 spots from 65 wholesome chickens and the average spectrum of 1850 spots from 74 systemically diseased chickens were then obtained. The two plots in *Fig. 3* show these averaged spectra and the standard deviations for wholesome and systemically diseased chickens, using both the LED and QTH line lights, respectively. *Figure 3* also shows the difference spectra between the average wholesome chicken spectrum and the average systemically diseased chicken spectrum using each type of line lights. From the difference spectra, the areas of greatest difference are clearly observable at the 413, 472, 515, and 546 nm wavelengths for the LED lights, and at the 465, 515, and 546 nm wavelengths for the QTH lights. Therefore, these wavelengths were selected as the key wavelengths for each corresponding light source.

A ratio method was developed to account for the potential effect on relative reflectance measurements from variations in lighting condition and distance between optical system and objects. A reference wavelength was selected and the ratio of the relative reflectance at this wavelength to that at each of the key wavelengths was calculated, in order to minimise the effect of lighting condition. At the 626 nm wavelength, the average spectral reflectance was observed to be greatest and the difference between average wholesome reflectance and average systemically diseased reflectance was relatively low (*Fig. 3*). This indicated that the image at this wavelength would be brighter and steadier than at other wavelengths. This wavelength was thus selected as the reference wavelength, and the ratio of relative reflectance between each key wavelength I_k and the reference wavelength I_r was calculated as follows

$$F_{k/r} = \frac{I_k}{I_r} \quad (3)$$

Therefore, four image features, $F_{413/626}$, $F_{472/626}$, $F_{515/626}$, $F_{546/626}$, were generated for each pixel of a scanned line using the LED line lights; and three image features, $F_{465/626}$, $F_{515/626}$, $F_{546/626}$, were generated for each pixel of a scanned line using the QTH line lights. These features were used as inputs for the image differentiation.

An algorithm was built to detect the entry of the chicken carcasses into, and their exit from, the camera field of view, and to determine the region of interest for each carcass. As shown by the contour maps in *Fig. 4*, the reflectance from the wings of a chicken was lower than that from other areas because of shadows and irregular surfaces. Eliminating the chicken wing areas from consideration increased the differentiation accuracy that was achieved (Yang *et al.*, 2005b). Using the algorithm to scan only the region of interest simplified image differentiation and reduced computational and memory management burdens for the computer; thus increasing computation speed for online inspection. The region of interest was considered to be the region encompassing the chicken thighs and main body (*Fig. 4*).

When a line was scanned, the average relative reflectance at 626 nm was calculated for the top 30 pixels (*Fig. 5*), or uppermost 16·50 mm. Empirically, when the average reflectance at 626 nm increased above 0·05, then the region of interest of the carcass had reached the field of view and subsequent line-scans were acquired for differentiation for the carcass. Acquisition was stopped when the average reflectance of the carcass detection length fell below 0·05 (*Fig. 5*). This method was applied to images acquired using both types of line lights.

2.5. *Fuzzy logic-based differentiation algorithm development*

In this study, fuzzy logic was applied to develop the algorithm to differentiate between images of wholesome and systemically diseased chickens. For algorithm development, the Fuzzy Logic Toolbox version 2.1.3 of MATLAB was used (MathWorks, Natick, MA, USA). The image features were used as fuzzy set inputs to produce a discrete output for decision-making.

In the first step, fuzzy logic mapped the inputs of fuzzy set (*i.e.* image feature in this study) to degrees of

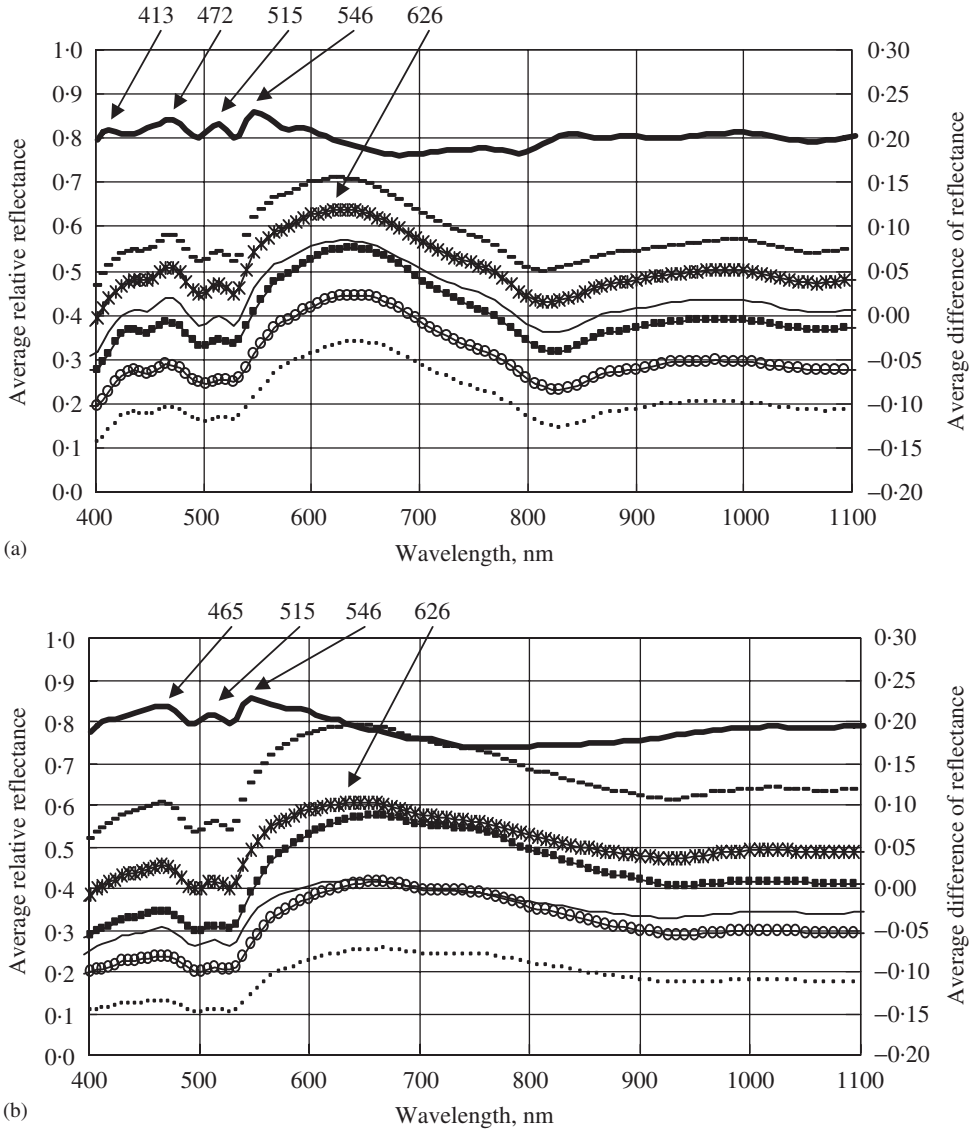

Fig. 3. Spectrum of relative reflectance for (1) wholesome chickens: average plus one standard deviation (■, wh+std), average (—✳—, wh), average minus one standard deviation (——, wh−std); (2) systemically diseased chickens: average plus one standard deviation (—■—, sys+std), average (—○—, sys), average minus one standard deviation (■, sys−std); and spectrum of (3) difference between wholesome and systemically diseased chickens (▬, wh-sys): (a) light-emitting-diode lights; (b) quartz–tungsten–halogen lights

the fuzzy membership ranging from zero to one, using the membership functions (Heske & Heske, 1996). To define membership functions, the image features of the 1625 spots of wholesome chickens and 1850 spots of systemically diseased chickens, used for key and reference wavelength selection, were calculated to obtain the average and standard deviation values for wholesome and systemically diseased chickens in each image feature, respectively. Each image feature had two corresponding input membership functions: a wholesome function and a systemically diseased function. Using the average and standard deviation values calculated above, the membership functions for each image feature were built (*Fig. 6*). The feature value for systemically diseased was usually lower than that for wholesome (*Figs 3* and *4*). Thus, in *Fig. 6*, the fuzzy degree for the systemically diseased function was equal to one when the image feature value was equal to the average ratio A_s or lower, and then decreased linearly to zero when the image feature was equal to or higher than the average A_s plus one standard deviation S_s. Conversely, in *Fig. 6*, the fuzzy degree for the wholesome function was equal to zero when the image feature value was equal to the average ratio A_w minus one standard

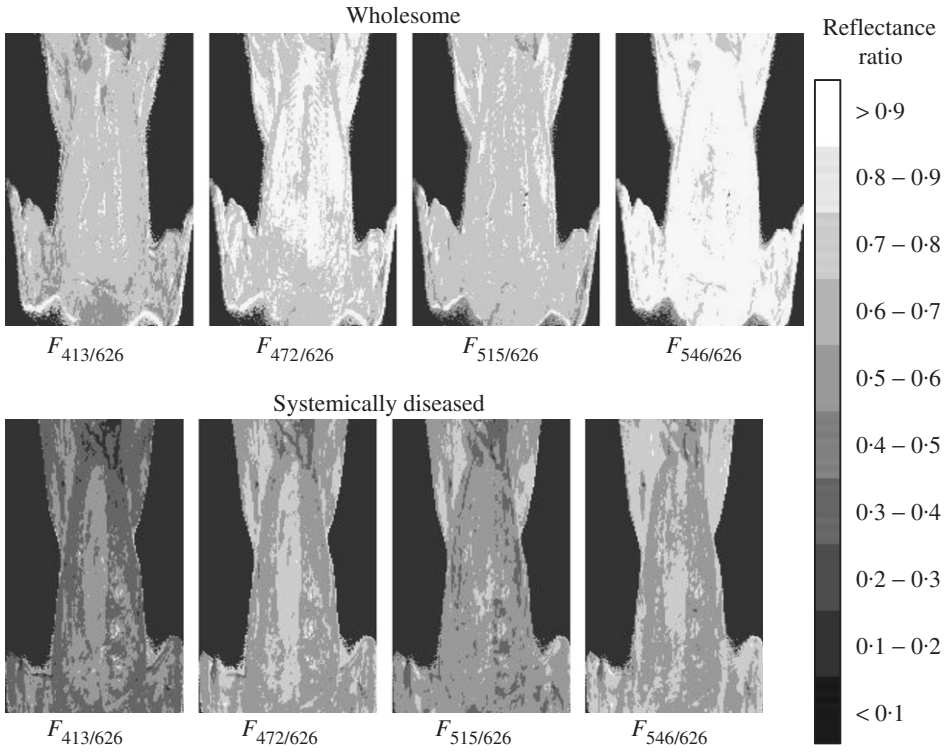

Fig. 4. Contour maps for wholesome and systemically diseased chickens by the light-emitting-diode line lights; $F_{k/r}$ for the ratio of relative reflectance between each key wavelength k and the reference wavelength r

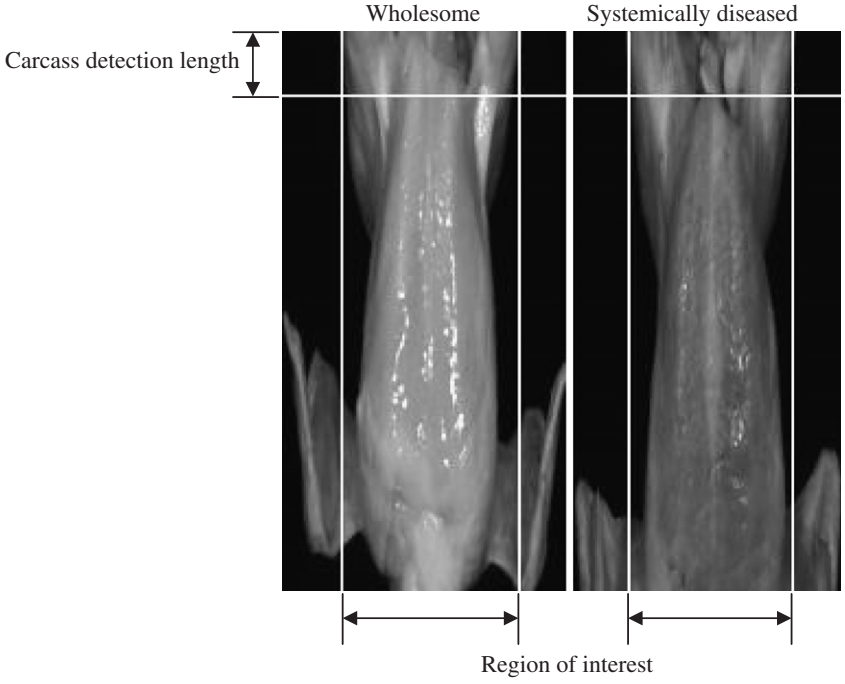

Fig. 5. Scheme to detect coming and leaving of chicken carcass and to determine the region of interest

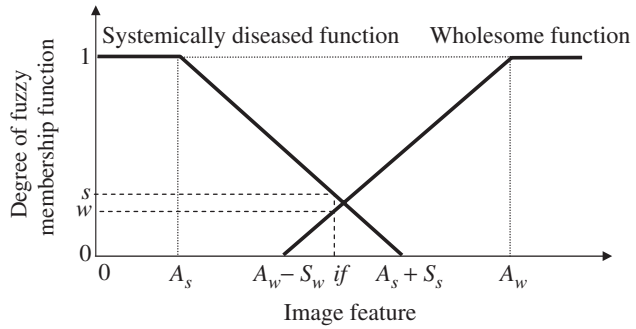

Fig. 6. The input fuzzy membership functions to map or fuzzify image feature inputs (i_f) to the fuzzy degrees of membership functions (w) and (s), for each image feature using the average relative reflectance ratios for 1625 wholesome sample spots (A_w) and 1850 systemically diseased sample spots (A_s) and the standard deviation for wholesome (S_w) and systemically diseased (S_s) sample spots

deviation S_w or lower, and then linearly increased to one when the image feature was equal to or higher than the average ratio A_w. Therefore, in the first step, each image feature input i_f could obtain two fuzzy degrees of membership functions, w for wholesome and s for systemically diseased (*Fig. 6*).

At the second step, two fuzzy rules were created to apply fuzzy membership functions (*Fig. 6*), for fuzzy operation as follows:

$$\text{If (every if is wholesome) then (chicken is wholesome, } w') \quad (4)$$

$$\text{If (every if is systemically diseased) then (chicken is systemically diseased, } s') \quad (5)$$

To execute the rules (*Fig. 6*), all of the fuzzy degrees from the wholesome function were compared and all of the fuzzy degrees from the systemically diseased function were compared to find the minimum fuzzy degrees, w' and s', respectively, to satisfy the above fuzzy rules. For the images collected using the LED line lights, there would be four fuzzy degrees for wholesome and four fuzzy degrees for systemically diseased since there were four image features for these images. For the images collected using the QTH line lights, there would be three fuzzy degrees for wholesome and three fuzzy degrees for systemically diseased since there were three image features for these images.

Then, in the next step for defuzzification, the fuzzy degrees of w' and s' were compared to make a decision output D_o. There were n image features for different light sources: n was four if using the LED line lights, and three if using the QTH line lights. The fuzzy engine was thus built as follows

$$D_o = f\ (\max\ [\min\ \{w_1 \ldots w_n\},\ \min\ \{s_1 \ldots s_n\}]) \quad (6)$$

The discrete decision output of D_o would be one when s' was higher than w', zero when w' was higher than s', and 0·5 when w' was equal to s'. The output is one for existence of systemic disease, zero for non-existence of systemic disease (*i.e.* the evidence of being wholesome), and 0·5 for uncertainty of decision.

To investigate the spatial variability while analysing spectrum data, four image features of each pixel from the scanned line were used to run the above fuzzy logic algorithm. Thus, each pixel provided one decision output. Two methods were tested for differentiation after the entire region of interest of a chicken carcass was scanned. In the first method, the decision outputs from all of the pixels in a scanned chicken carcass were averaged to represent the chance for the carcass to be systemically diseased. The higher the chance, the more confidently the chicken is condemned. In the second method, the decision outputs from all the chicken pixels of each individual line-scan were averaged. If the average output was higher than 0·5, *i.e.* more certain for existence of systemic disease symptom, the line was marked as a suspected line. The total number of suspected lines for the entire carcass was counted and analysed as the final output for the carcass.

The fuzzy logic-based algorithm was developed based on the first image set. Each of two differentiation methods based on the developed algorithm was tested using the first and second image sets, respectively. The image sets were collected at different times, independently from each other.

3. Results and discussion

Although previous studies (Yang *et al.*, 2005a, 2005b) have demonstrated that QTH lights can be used successfully for identifying wholesome and systemically diseased chicken conditions, comparisons of the spectral measurements for QTH and LED lights, as shown in *Fig. 1*, indicated that the LED lights provide higher intensity illumination at shorter wavelengths, *i.e.* the region from 400 to 550 nm. This region includes multiple wavelengths that have been found to reflect the presence of several myoglobin species that are found in chicken meat and closely correlated to chicken condition; consequently, these wavelengths are useful for identifying chicken conditions (Liu & Chen, 2001). In this study, determining key wavelengths for identifying chicken conditions using the LED lights resulted in four key wavelengths that included one in this lower 400–500 nm

region. Using the QTH lights resulted in only three key wavelengths.

Figure 3 shows the average spectra for wholesome and systemically diseased chickens obtained using (a) LED lights and (b) QTH lights. The average wholesome chicken spectrum shows higher relative reflectance than the average systemically diseased chicken spectrum across all wavelengths. For the LED lights, there is no overlap between the one-standard-deviation envelopes around the average wholesome and average systemically diseased chicken spectrum. In contrast, there is significant overlap when using the QTH lights. Around 700 nm, the one-standard-deviation envelope for the average wholesome chicken spectrum very nearly coincides with the average systemically diseased chicken spectra, and the one-standard-deviation envelope for the systemically diseased chicken spectrum comes similarly close to the average wholesome chicken spectrum.

The relative reflectance ratios calculated with the key wavelengths were used as image features. *Figure 7* shows the average ratio values for wholesome and systemically diseased chicken using (a) the four LED key wavelengths and (b) the three QTH key wavelengths. When using the LED lights, the average wholesome and average systemically diseased ratio values are each always outside the one-standard-deviation range of the

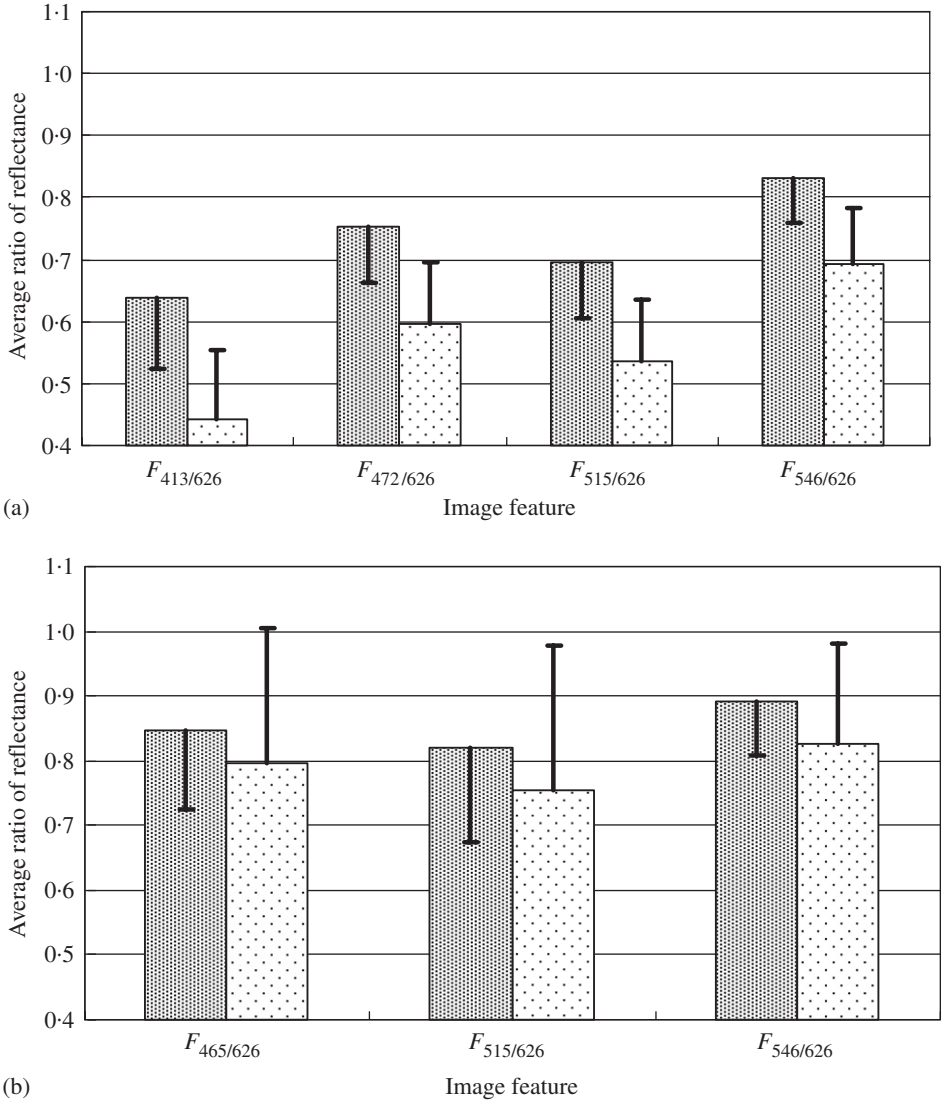

Fig. 7. The average, average minus one standard deviation (for ▨, wholesome), and average plus one standard deviation (for ⬚, systemically diseased) of all image features $F_{k/r}$ (the ratio of relative reflectance between each key wavelength k and the reference wavelength r) from 1625 sample spots of 65 wholesome chickens and 1850 sample spots of 74 systemically diseased chickens: (a) light-emitting-diode lights; (b) quartz-tungsten-halogen lights

other chicken condition, for all four image features. In comparison, the one-standard-deviation ranges of the ratio values are 7% to 180% larger for the QTH lights, and consequently the average wholesome and average systemically diseased ratio values are each always inside the one-standard-deviation range of the other chicken condition, for all three image features. The use of QTH lights to distinguish wholesome and systemically diseased chickens presents greater difficulties than the use of LED lights. Thus, only the images taken using the LED line lights were used for the evaluation of fuzzy logic-based differentiation methods.

The results from using the first differentiation method with the first image set show that wholesome and systemically diseased chickens can be easily distinguished from each other according to the value of the average decision output for each chicken image, as shown in *Fig. 8*. The average decision output was always correctly high for systemically diseased chickens (above 0·50) and always unmistakably low for wholesome chickens (below 0·5). Therefore, when a chicken was assigned a greater than 50% of chance of being systemically diseased chickens (*i.e.* higher than 0·50 of average decision output), that carcass was condemnable without risk of economic loss. The chickens that were assigned a less than 50% of chance of being systemically diseased (*i.e.* lower than 0·50 of average decision output) were identified as wholesome with respect to systemic disease conditions. The results indicated that, by applying the value of 0·50 as the threshold, the fuzzy logic-based differentiation algorithm successfully differentiated systemically diseased chickens from wholesome chickens. The results indicated that this method of calculating the average pixel decision output value, for all the chicken-surface pixels in the chicken image, successfully differentiated the 65 wholesome chickens and 74 systemically diseased chickens in the first image set.

The second image set was used to test the first differentiation method. For this independent data set, the average pixel decision output was again found to be a good indicator of chicken condition. *Figure 9* shows the results for the second image set, for which the 0·50 threshold value was successfully used to separate 48 wholesome chickens and 42 systemically diseased chickens.

Figure 10 shows the results for the second differentiation method using the first image set. For this method, each line in the image was analysed to find the average decision output for all the chicken-surface pixels within that line, and then the average value for the line was calculated. The line was identified as a "suspect" line if its average was greater than the 0·5 threshold value. All the scan lines of the chicken image were analysed in this way. The results showed that the images of wholesome chickens always included fewer than 40 suspect lines. Thus, line-by-line counting of suspect lines enabled a chicken image to be identified as systemically diseased as such as soon as more than 40 suspect lines were counted, without the need to continue acquisition and analysis of further lines for that image. By using this method, 71 out of 74 systemically diseased chickens and all 65 wholesome chickens in the first image set were correctly identified. For the independent second image set, this

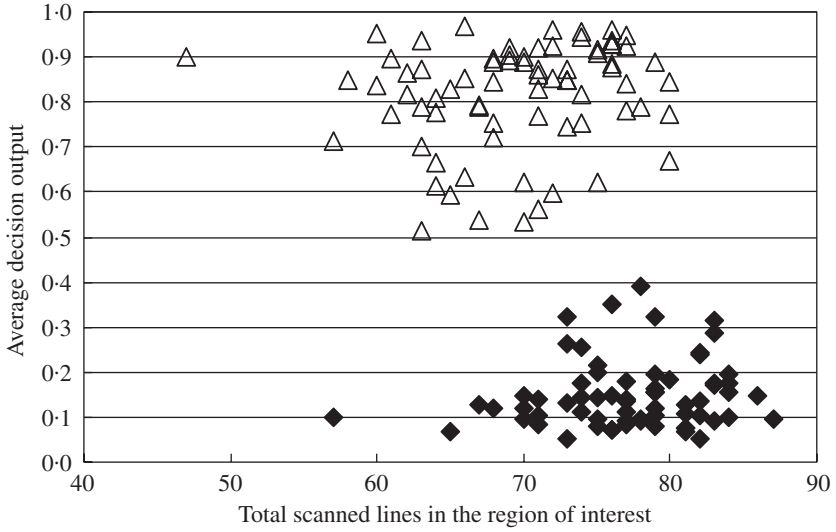

Fig. 8. The average decision outputs for wholesome and systemically diseased chickens by the first differentiation method for the first image set of 65 wholesome chickens (◆) and 74 systemically diseased chickens (△)

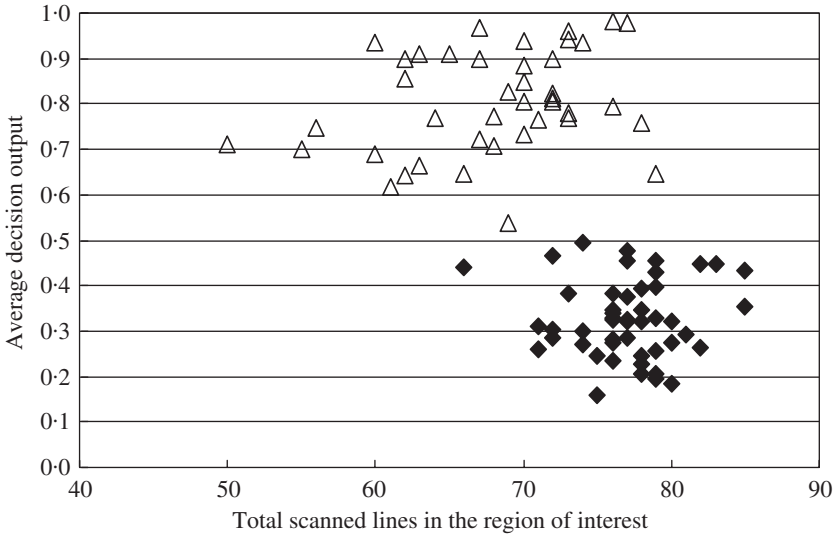

Fig. 9. The average decision outputs for wholesome and systemically diseased chickens by the first differentiation method for the second image set of 48 wholesome chickens (◆) and 42 systemically diseased chickens (△)

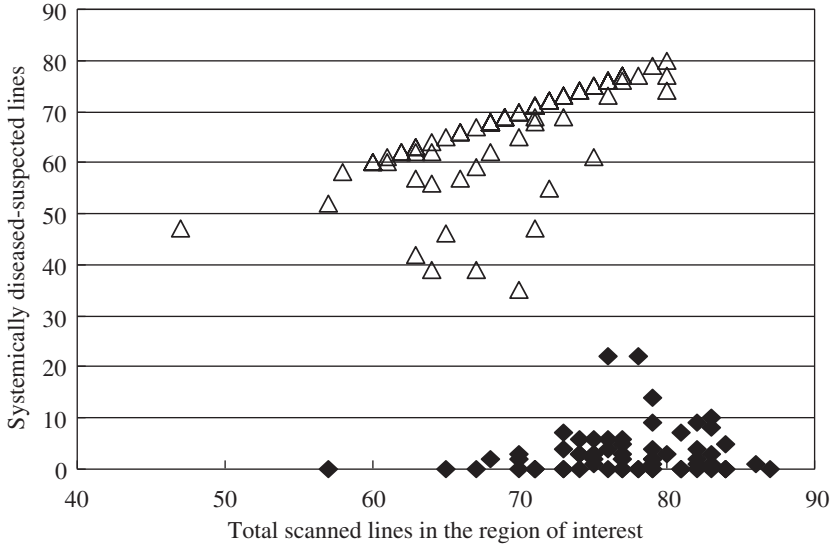

Fig. 10. The number of systemically diseased-suspected lines for wholesome and systemically diseased chickens by the second differentiation method for the first image set of 65 wholesome chickens (◆) and 74 systemically diseased chickens (△)

line-count method successfully differentiated all 42 systemically diseased chickens and all 48 wholesome chickens, as shown in *Fig. 11*.

The results of the line-count method demonstrate one of the advantages of line-scan imaging for real-time operations: sometimes a decision can be made before the entire chicken has been scanned, which reduces the computational effort and processing time required. In *Figs 10* and *11*, the distribution of wholesome and systemically diseased chicken images is shown according to the number of suspect lines in the image *versus* the number of lines composing the region of interest in that image. Wholesome chickens tended to be larger than systemically diseased chickens, with the smallest wholesome chicken images containing 57 and 66 line-scans, from the first and second image sets, respectively.

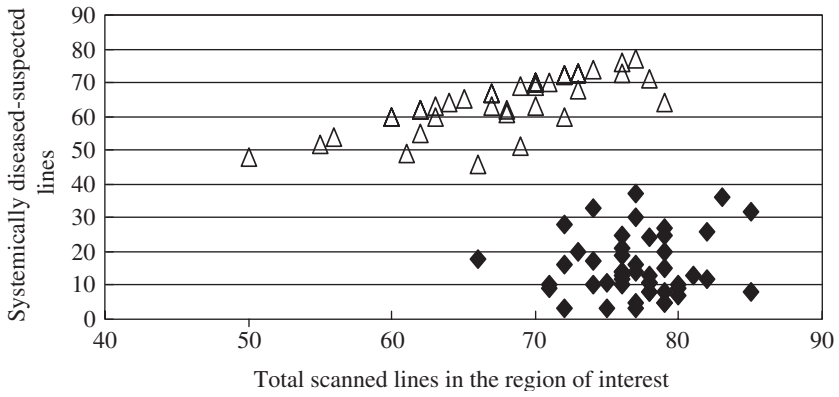

Fig. 11. The number of systemically diseased-suspected lines for wholesome and systemically diseased chickens by the second differentiation method for the second image set of 48 wholesome chickens (◆) and 42 systemically diseased chickens (△)

Wholesome chicken images had significantly fewer suspect lines than systemically diseased chicken images, but it was also noted that among wholesome chicken images, the smallest did not necessarily have the fewest suspect lines and the largest did not necessarily have the greatest number of suspect lines. The greatest number of suspect lines found for any wholesome chicken in the first set was 22, and that for any wholesome chicken in the second set was 37.

For systemically diseased chicken images, the total number of line-scans in the region of interest ranged from 47 to 80 in the first image set and from 50 to 79 in the second image set. Above 95% of the systemically diseased chicken images in the first set had more than 40 suspect lines, and all of the systemically diseased chicken images in the second set had more than 40 suspect lines. Thus, a count of 40 suspect lines is a reasonable threshold for use in differentiating systemically diseased chickens from wholesome chickens, for the imaging system parameters and processing line speed in this study. Changes in imaging parameters or processing speed would affect the threshold values (0·5 decision output threshold and 40-line count) but the methodology would remain valid.

The results show that this hyperspectral imaging system would take 90 to 160 scan lines to complete an image of a chicken carcass from wingtip to wingtip. The imaging speed of the system is high enough to present a clear image for differentiation. However, the results also showed that it is not necessary to consider the lines scanned from the wing areas because the reflectance from the wings was often interrupted by shadows and irregular surfaces. Furthermore, for a real-life processing plant situation, the wings of chickens hung side by side on the processing line often overlap each other, making full wingtip-to-wingtip imaging difficult. Precise identification of the starting and ending line for each complete carcass is difficult and unnecessary, and increases processing time. Therefore, it is practical to scan only the thighs and body of each chicken instead of the entire chicken from wingtip to wingtip.

The nearly 100% of accuracy achieved using the two differentiation methods strongly indicates that the key wavelengths of 413, 472, 515, and 546 nm were appropriately selected for differentiating systemically diseased chickens from wholesome chickens. Having determined key wavelengths to use, a line-scan hyperspectral imaging system such as the one in this study can then be operated as a multispectral imaging system by reducing the high number of waveband channels used to just the selected few. In this study, hyperspectral images were acquired using 103 channels, but by limiting the system to multispectral operation using only the selected five (four key wavelengths and one reference wavelength) channels, imaging speed could be significantly increased. Such capacity for rapid operations is crucial to implementing imaging systems for online poultry carcass inspection. In addition, the hyperspectral/multispectral imaging system used in this study also can be easily implemented by changing camera-control software settings. This eliminates the usual requirements for cross-system calibration between separate hyperspectral and multispectral systems when transferring the methods developed from hyperspectral wavelength selection.

The fuzzy logic-based algorithm, on which these two differentiation methods based, can be applied to other populations of chickens (varying in season, geography, or growth conditions). Inclusion of additional populations requires the collection of additional samples to account for additional variations encountered, resulting

in minor modifications to the fuzzy membership functions.

4. Conclusions

In this study, a hyperspectral line-scan imaging system was used to acquire images of 113 wholesome and 114 systemically diseased chickens in two sets, 65 wholesome and 74 systemically diseased for the first image set, and 48 wholesome and 42 systemically diseased for the second image set. The chicken carcasses were hung on a line of shackles moving at a speed of 70 birds per minute. Light-emitting-diode (LED) line lights were selected as the appropriate light source since the difference of relative reflectance between wholesome and systemically diseased chickens is more significant and the reflectance for the shorter wavelengths is higher than that resulting from quartz–tungsten–halogen (QTH) illumination. Spectral analysis showed that, among the 103 available wavelengths from 395 to 1138 nm, the four wavelengths at 413, 472, 515, and 546 nm are the key wavelengths when using the LED line lights. They were identified from the peaks of the curve for the difference spectra between wholesome and systemically diseased chickens. The wavelength of 626 nm was selected as the reference wavelength for calculating band ratios with the key wavelengths, to use as input image features for the fuzzy logic decision algorithm. Four image features were thus obtained, one for each key wavelength. The region of interest in the chicken images was defined as the thighs and body of the chicken.

A fuzzy logic-based algorithm was developed to differentiate between images of wholesome and systemically diseased chickens. For each scanned line, four image features calculated for single pixels were used as inputs to the fuzzy logic algorithm to obtain a discrete decision output, indicating the existence of systemic disease. Two differentiation methods were investigated in this study. For the first method, the average decision output was calculated for all pixels on the chicken surface within all scanned lines of the region of interest. The fuzzy logic algorithm accurately differentiated systemically diseased chickens from wholesome chickens: when the average pixel decision output was higher than 0·50, the chicken was identified as being systemically diseased. For the second method, the average decision output was calculated for all pixels on the chicken surface of each scanned line, and the number of lines in which the average output was higher than 0·50 were counted for the chicken image. The results showed that when the count of suspect lines was higher than 40, the carcass could be identified as being systemically diseased.

The results using the first differentiation method show that the use of key wavelength band ratios as image features is effective in identifying systemically diseased chicken surfaces. The line-scan imaging system achieved 100% accuracy in identifying two sets of wholesome and systemically diseased chickens with the use of only five wavelengths (four key wavelengths and one reference wavelength), demonstrating ideal speed and simplicity for practical application in a processing environment. In comparison, the second differentiation method correctly identified 71 out of 74 systemically diseased chickens in the first image set, demonstrating that the line-count method can still achieve significant accuracy (96%) while further increasing processing efficiency by eliminating the need to scan the entire Region of Interest for every chicken image. Further investigation is needed to determine variables that may be adjusted with circumstances to optimise the use of the line-count differentiation method.

References

Bjuggren M; Krummenacher L; Mattsson L (1997). Noncontact surface roughness measurement of engineering surfaces by total integrated infrared scattering. Precision Engineering, **20**(1), 33–45

Chen Y R; Massie D R (1993). Visible/near-infrared reflectance and interactance spectroscopy for detection of abnormal poultry carcasses. Transactions of the ASAE, **36**(3), 863–869

Christensen L K; Bennedsen B S; Jorgensen R N; Nielsen H (2004). Modelling nitrogen and phosphorus content at early growth stages in spring barley using hyperspectral line scanning. Biosystems Engineering, **88**(1), 19–24

Connelly J P; Botchway S W; Kunz L; Pattison D; Parker A W; MacRobert A J (2001). Time-resolved fluorescence imaging of photosensitiser distributions in mammalian cells using a picosecond laser line-scanning microscope. Journal of Photochemistry and Photobiology A: Chemistry, **142**(2–3), 169–175

Heske T; Heske J N (1996). Fuzzy Logic for Real World Design. Annabooks, San Diego, CA, USA

Keskin M; Dodd R B; Han Y J; Khalilian A (2001). Comparison of different types of light sources for optical cotton mass measurement. Transactions of the ASAE, **44**(3), 715–720

Lawrence K C; Park B; Windham W R; Mao C (2003). Calibration of a pushbroom hyperspectral imaging system for agricultural inspection. Transactions of the ASAE, **46**(2), 513–521

Liu Y; Chen Y R (2001). Analysis of visible reflectance spectra of stored, cooked and diseased chicken meats. Meat Sci., **58,** 395–401

Park B; Lawrence K C; Windham W R; Buhr R J (2002). Hyperspectral imaging for detecting fecal and ingesta contamination on poultry carcasses. Transactions of the ASAE, **45**(6), 2017–2026

Polder G; van der Heijden G W A M; Young I T (2002). Spectral image analysis for measuring ripeness of tomatoes. Transactions of the ASAE, **45**(4), 1155–1161

USDA (1996). Pathogen Reduction: Hazard Analysis and Critical Control Point (HACCP) Systems. Final Rule. Fed. Reg. 61: 28805-38855. USDA, Washington, DC, USA

USDA (2005). Standard Operating Procedures for Notification and Protocol Submission of New Technologies. USDA, Washington, DC, USA

Yang C-C; Chao K; Chen Y R (2005a). Development of multispectral imaging processing algorithms for identification of wholesome, septicemia, and inflammatory process chickens. Journal of Food Engineering, **69**(2), 225–234

Yang C-C; Chao K; Chen Y R; Early H L (2005b). Systemically diseased chicken identification using multispectral images and region of interest analysis. Computers and Electronics in Agriculture, **49**(2), 255–271